



# Patient MW: transient visual hemi-agnosia

Thomas Decramer<sup>1,2</sup> · Elsie Premereur<sup>2</sup> · Lieven Lagae<sup>3</sup> · Johannes van Loon<sup>1</sup> · Peter Janssen<sup>2</sup> · Stefan Sunaert<sup>4</sup> · Tom Theys<sup>1</sup>

Received: 14 November 2018 / Revised: 21 December 2018 / Accepted: 3 January 2019 / Published online: 7 January 2019  
© Springer-Verlag GmbH Germany, part of Springer Nature 2019

## Abstract

The concept of functional modularity in human visual processing was proposed 25 years ago with the distinction between a ventral pathway for object recognition and a dorsal pathway for action processing. Lesions along these pathways yield selective deficits. A 15-year-old patient (MW) presented with a seizure due to a lesion in the left occipitotemporal cortex. Surgical resection of the lesion was performed with sparing of the classic language areas and visual fields. Postoperatively MW had great difficulty reading and had a specific agnosia for more complex visual stimuli in the right hemifield. No deficit was seen for lower level visual discrimination tasks. Gradual improvement of hemi-agnosia was paralleled by slower reaction times reflecting a speed–accuracy trade-off. Absolute reading speed improved markedly over time, doubling at 6 weeks. MW fully recovered after 18 months. Postoperative functional Magnetic Resonance Imaging (fMRI) illustrated an overlap of the lesion with object and word processing areas. Diffusion Tensor Imaging showed damage to the white matter tracts [inferior fronto-occipital fasciculus and inferior longitudinal fasciculus (ILF)] interconnecting ventral temporal areas. A transient higher order deficit can result from a disruption of the neural network supporting visual word and object processing. Most visual system research has focused on cortical areas, while the underlying subcortical network received much less attention. We believe that white matter tracts, in particular the ILF, play a critical role in object perception by connecting visual areas along the ventral visual stream. Lesions of the ILF should be taken into consideration in agnosia.

**Keywords** Occipitotemporal cortex · Visual agnosia · Visual pathways · Visual perception · Reading · Visual processing · Ventral visual pathway

## Introduction

About 25 years ago, the concept of functional modularity in human visual processing was proposed with the distinction between a ventral pathway for object recognition and a dorsal pathway for action processing [1]. This regional specialization theory was further supported by monkey research

[2, 3], lesion studies [4–13], positron emission tomography (PET) [14, 15], and fMRI studies [16]. Human fMRI studies have provided substantial evidence that the occipitotemporal cortex is organized according to specific object classes or features, similar to the inferior temporal cortex (ITC) in the monkey.

## Case

A 15-year-old right-handed patient (MW) was admitted with a secondary generalized seizure. MRI revealed a T2 hyperintense lesion without contrast enhancement in the left occipitotemporal cortex, located in Brodmann area (BA) 37, with a slight extension into BA 20 (MNI space coordinates:  $x - 36$  to  $-60$  mm,  $y - 52$  mm to  $-78$  mm,  $z 8$  mm to  $-16$  mm) (Fig. 1). Clinical and ophthalmological examination was normal. A verb generation task-based fMRI showed a left-lateralized language system. The lesion was located just

✉ Tom Theys  
tom.theys@uzleuven.be

<sup>1</sup> Department of Neurosciences, Research Group Experimental Neurosurgery and Neuroanatomy, KU Leuven, Herestraat 49, 3000 Leuven, Belgium

<sup>2</sup> Laboratory for Experimental Neuro- and Psychophysiology, Department of Neurosciences, KU Leuven, Leuven, Belgium

<sup>3</sup> Department of Pediatrics, University Hospitals Leuven, Leuven, Belgium

<sup>4</sup> Department of Imaging and Pathology, Translational MRI, KU Leuven, Leuven, Belgium

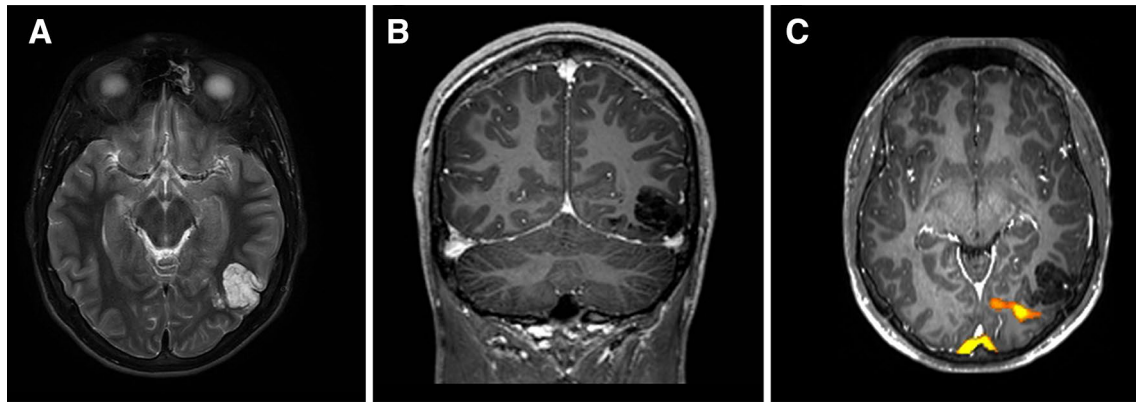


**Fig. 1** Preoperative MR imaging of the brain. **a** Axial T2-weighted image shows a hyperintense lesion in the left occipitotemporal region. **b** Coronal T1-weighted imaging with gadolinium. **c** fMRI retinotopic mapping: the lesion is located just anterior to the lower order visual areas

anterior to the retinotopic lower order visual areas (Fig. 1c). Surgical resection was performed and pathology revealed a dysembryoplastic neuroepithelial tumor (DNET). In the first days after surgery, the patient could detect simple visual stimuli in the contralateral hemifield, but was unable to recognize more complex shapes. He was not aware of this deficit and did not report visual symptoms. Reading, particularly long words, was dramatically impaired.

## Methods

Written informed consent was obtained from the patient and his parents for further psychophysical testing and advanced imaging according to study s61263, approved by the local ethical committee.

### Stimuli and testing

Visual categorization tasks were performed in a stereoscope with continuous eye movement tracking (ISCAN, 125 Hz), ensuring fixation in an electronically defined window throughout the experiment. Images from two LCD monitors were presented to the eyes with the use of customized mirrors at a viewing distance of 56 cm (1 pixel = 0.028°). Stimuli were presented either in both visual hemifields, either on the horizontal meridian (9.5° lateral from the fixation point) or in the lower visual quadrant (9.5° lateral and 4.5° below the fixation point). Presentation in the lower visual quadrant excluded any interference from a possible ‘pie-in-the-sky’ visual field deficit. Stimulus size varied between 7° and 8.5°. The fixation point (0.14 × 0.14°) was located in the center of the screen. The patient was instructed to report the presence of the target or distractor stimulus by means of a left or right button press. All stimuli were presented on the screen for a fixed period, and the patient could only respond

after stimulus offset. Trials were aborted if fixation was not maintained. Each task was preceded by a short training session of 30 trials. Tasks were completed after 100 correct trials per hemifield.

Extensive psychophysical testing included different visual categorization tasks for 1 week (1w), 6 weeks (6w) and 3 months (3m), and 18 months (18m) after surgery. The proportion of correct trials and reaction times (RTs) were calculated at all time points.

### Visual stimuli

In the object recognition task, the patient had to discriminate between achromatic photographs of birds (target) and other stimuli (distractors: other animals, fruits, bodies, faces, objects, and sculptures) displayed in the lower visual quadrants (stimulus size 7°) [17]. Birds appeared randomly in 10% of trials. All stimuli were presented for 800 ms.

The LOC localizer categorization task consisted of objects (target: shapes and outlines) and scrambled objects (distractors: scrambled shapes or outlines) presented in the lower visual quadrants. Stimuli (size 8.5°) were presented for 800 ms.

Low-level visual processing was assessed by discriminating straight lines (/, \) and simple curved (C, ∩) stimuli, presented in the left and right visual hemifield. Stimuli (size 8.5°) were presented for 800 ms.

Motion perception was tested at 6w using dynamic random dot stimuli with vertical and horizontal motion at different coherences (i.e., the percentage of dots defining motion). Stimuli were shown for 1800 ms.

Stereopsis was tested at 3m using foveally presented disparity-defined stimuli in a 3D categorization task (Verhoef et al. 2016). A stereo-acuity test to evaluate local stereopsis was followed by a 3D-structure discrimination task using stimuli with different coherences.

## Reading

Reading was assessed 1w, 6w, and 18m after surgery using the same 128-word text from a local newspaper printed on a blank sheet (A4, Arial font size 12, double line spacing). Reading was audio-recorded to evaluate reading speed and reading errors.

## Grasping

Grasping was filmed during a delayed visually guided grasping task in which the patient had to fixate and grasp a small sphere presented in both hemifields.

## Statistical analysis

Errors were defined as incorrectly categorized stimuli, hits as correctly detected targets (% hits was calculated based on all the presented targets) and false alarms as incorrect detection of the target (% false alarms based on all the presented distractors). The sensitivity index ( $d'$ ) was calculated for every experiment on the  $z$ -scored hit rates and false alarm rates [ $d' = z(\text{hit rate}) - z(\text{false alarm rate})$ ], with a higher  $d'$  indicating better target detection. Reaction times (RTs), including the standard error of mean ( $\pm$  SEM), were calculated as the time difference between the go-signal and button press. Abort trials due to loss of fixation or early response were excluded. Custom made scripts (Matlab) were used for data analysis. Differences in RTs were calculated using Friedman's test.

## Anatomical and functional MRI

Preoperative fMRI (Philips Achieva 3T) was used to determine language lateralization and assess retinotopy. Post-operative fMRI was performed at 18m with three different localizers: an LOC localizer (comparing objects and outlines to scrambled objects and outlines), an FFA localizer (comparing faces and scrambled faces), and a VWFA localizer comparing words and phase-scrambled words. Preprocessing was performed using FMRIPREP version 1.1.4, a Nipype-based tool [18]. Physiological noise regressors were extracted applying CompCor [19]. Frame-wise displacement [20] was calculated for each functional run. SPM12 was used to identify task-specific activations at the single-subject level. Data were smoothed using SPM12 with a 6 mm FWHM Gaussian isotropic kernel. Each condition was modeled by a boxcar function convolved with a hemodynamic response function in the GLM. Noise regressors and frame-wise displacement were added to the model as covariates of non-interest. First-level T contrasts for “faces versus scrambled faces”, “objects versus scrambled objects” and “words versus scrambled words” were calculated and

thresholded at  $p < 0.05$  FWE corrected. Clusters with  $t$  values  $> 4.9$  were used for figures. Language fMRI was also repeated at 18m.

At 18m, diffusion tensor imaging was performed with along tract quantitative analysis, using Explore DTI [21]. The right inferior longitudinal fasciculus was segmented in 24 segments and the left (due to the lesion) in 15 corresponding segments. The inferior fronto-occipital fasciculus (IFOF) was bilaterally segmented in 18 segments. Non-parametric statistics (Kruskal–Wallis) were used to compare the FA values within one segment, with correction for multiple comparisons.

## Results

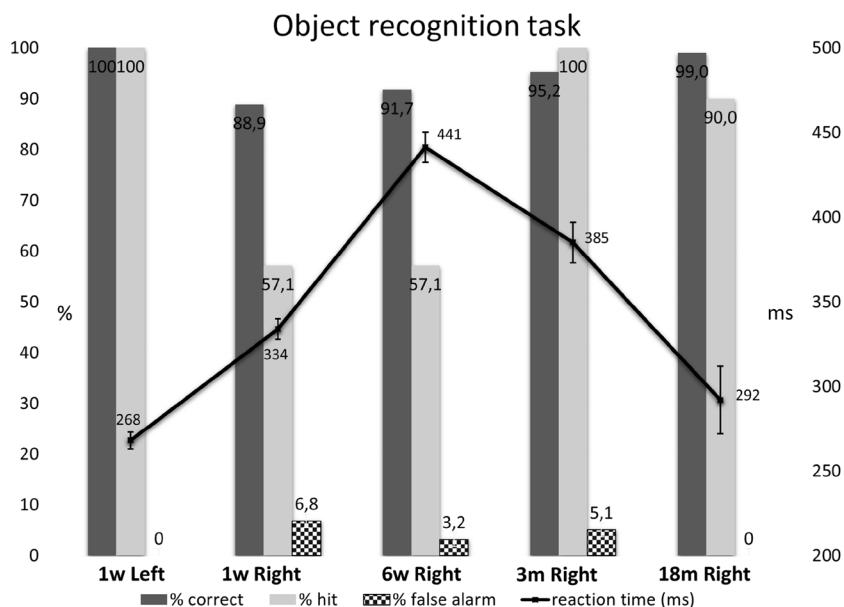
### Visual stimuli

At 1w, performance in the *object recognition* task was much worse for stimuli presented in the right hemifield ( $d'$  left 5.38,  $d'$  right 1.67). General performance as well as hit rate were lower for stimuli presented in the right lower quadrant (percent correct—left 100%; right 88.9%; percent hits—left 100%, right 57.1%), while the percentage of false alarms was higher (left 0%, right 6.8%). The patient responded significantly slower for stimulus presentations on the right side ( $334 \pm 6$  ms) compared to left ( $268 \pm 5$  ms; Friedman test for non-parametric repeated measures: 64;  $df = 1$ ,  $p < 0.001$ ). At 6w, a partial recovery of the deficit was present (91.7% correct; 57.1% hits,  $d' 2.04$ , false alarms 3.2%), whereas, at 3m, performance improved markedly (95.2% correct; 100% hits,  $d' 3.97$ ), although false alarms were still present (5.1%) (Fig. 2). RTs changed significantly over time: at 6w, RTs increased further compared to 1w ( $441 \pm 9$  ms), while at 3m, RTs decreased, but were still higher ( $385 \pm 12$  ms) than at 1w (Friedman test 60.62;  $df = 2$ ,  $p < 0.001$ ) (Fig. 2). Thus, improved performance for contralesional presentations was paralleled by slower RTs, indicating a speed–accuracy trade-off. At 18m, performance normalized and RTs recovered ( $292 \pm 20$  ms).

The patient performed remarkably well in line and curve orientation categorization in both visual hemifields ( $> 98\%$  correct, % hits: 100,  $d' > 4$ ). No difference in RTs was found for line stimuli presented in both hemifields (right:  $425 \pm 8.1$  ms; left:  $408 \pm 7$  ms; Friedman test 0.36;  $df = 1$ ;  $p = 0.55$ ), while the patient did react slightly slower for curved lines presented on the contralesional side ( $365 \pm 6$  versus  $388 \pm 5$  ms; Friedman test 8.33,  $df = 1$ ,  $p = 0.004$ ).

In the LOC localizer categorization task, performance was excellent in both the left and right lower visual quadrants at 1w (resp. 98 and 97% correct; 98 and 96% hits,  $d' 4.11$  and 4.47) but RTs were longer for stimuli in the right hemifield ( $428 \pm 9$  versus  $388 \pm 5$  ms; Friedman test 9.00,

**Fig. 2** Performance in the object recognition task during follow-up (at 1w, 6w, 3m, and 18m). All stimuli were presented in the lower visual quadrants. The percentage correct trials, hits, and false alarms are shown. Reaction times are shown in milliseconds [Y axis; right (ms)] on the curve with their standard error of mean (SEM)



$df=1$ ;  $p=0.0027$ ). RTs in the LOC localizer categorization task returned to normal at 6w ( $389 \pm 9$  ms; Friedman 6.67,  $df=1$ , and  $p=0.01$ ).

Motion perception at 6w was intact for both hemifields (percent correct >97%, % hits: >94%,  $d' > 4.4$ ). Finally, stereovision tested foveally at 3m was intact (% correct: 98; % hits: 96, and  $d' 4.4$ ).

## Reading

Absolute reading speed improved dramatically over time. At 1w, the patient was able to read the 128-word text in 180 s, while, at 6w, he could read the same text in 85 s. We noticed particular difficulties reading longer words, in which case the patient performed multiple saccades before making a

pronunciation attempt. At 18m reading, the 128-word text took 65 s.

## Grasping

In a simple visually guided grasping task, we did not observe any deficit. No subjective grasping difficulties were present, and the subject could perform fine motor commands in everyday life without any changes.

## Postoperative imaging

At the cortical level, structural MRI showed the resection encompassing Brodmann areas 37 and 20 at 6m (Fig. 3). At the subcortical level, imaging characteristics typical for late Wallerian degeneration (T2 hyperintensity and T1

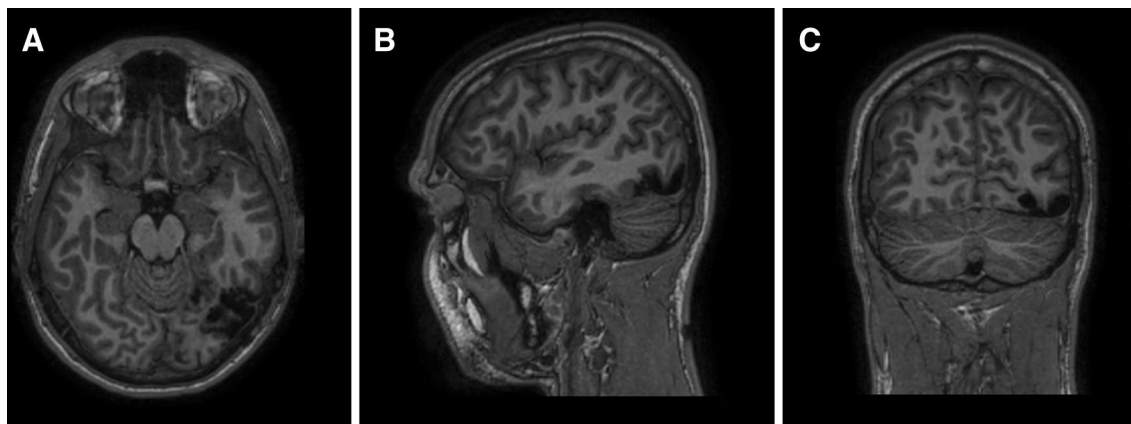


**Fig. 3** Postoperative MR imaging of the brain at 6 months, T1-weighted imaging. **a** Axial. **b** Sagittal. **c** Coronal

hypointensity) in the sagittal stratum (Fig. 4) were present at 18m. These changes even occurred in remote areas and were not present on the previous scans.

Language fMRI at 18m showed identical activations compared to the preoperative fMRI. The LOC localizer only showed activations in the contralesional hemisphere, at the homotopic location of the lesion (Fig. 5). The FFA localizer showed right-sided activations partly overlapping with LOC (Fig. 5). The VWFA localizer showed unilateral left-sided activations just anterior to the lesion (Fig. 5).

On qualitative DTI tracking, the posterior part of the left ILF could not be tracked (due to the presence of the lesion) (Fig. 6). On along tract analysis, all segments of the left ILF had decreased FA values compared to the right ILF. Over all segments combined the left ILF (FA  $0.44 \pm 0.05$ ) had a lower FA value compared to the right (FA  $0.56 \pm 0.02$ ) reflecting degeneration of the tract. The left IFOF also showed a significant decrease in FA values in its posterior segments (closer to the lesion); however, overall there was no statistical difference between the left (FA  $0.50 \pm 0.039$ ) and right IFOF (FA  $0.56 \pm 0.080$ ).

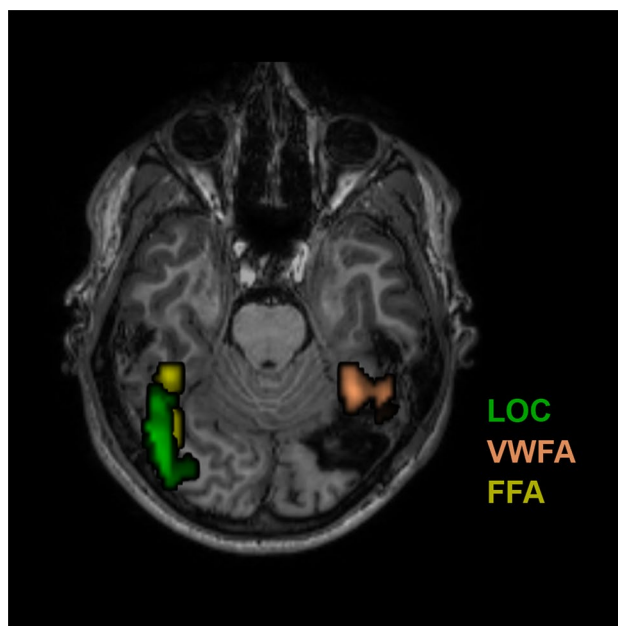


**Fig. 5** Functional MRI. LOC (green), VWFA (copper), and FFA (yellow) localizers were used in an fMRI session performed 18 months after surgery. LOC activation was not obtained on the side of the resection

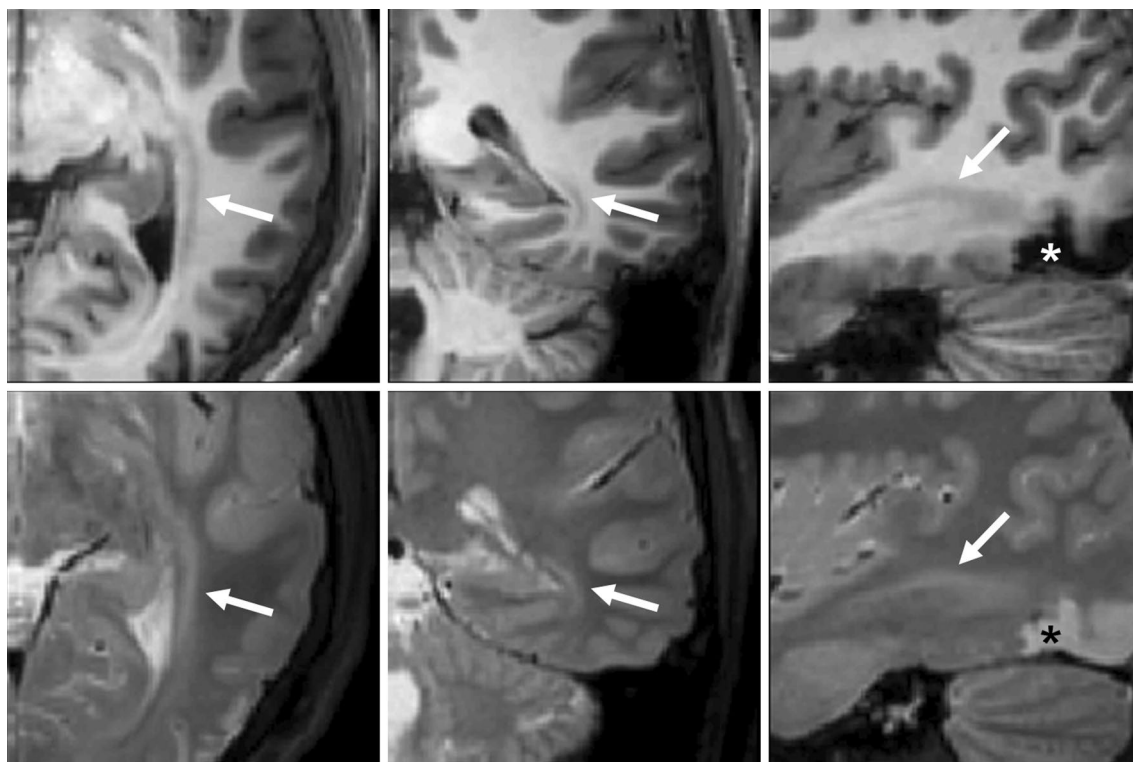


**Fig. 4** Structural MRI at 18 months. Upper panels: T1 weighted imaging (left: axial, center: coronal, right: sagittal), lower panels: FLAIR imaging (left: axial, center: coronal, right: sagittal) illustrates

late Wallerian degeneration of fiber tracts of the sagittal stratum (SS). Both the ILF and IFOF are located in the SS

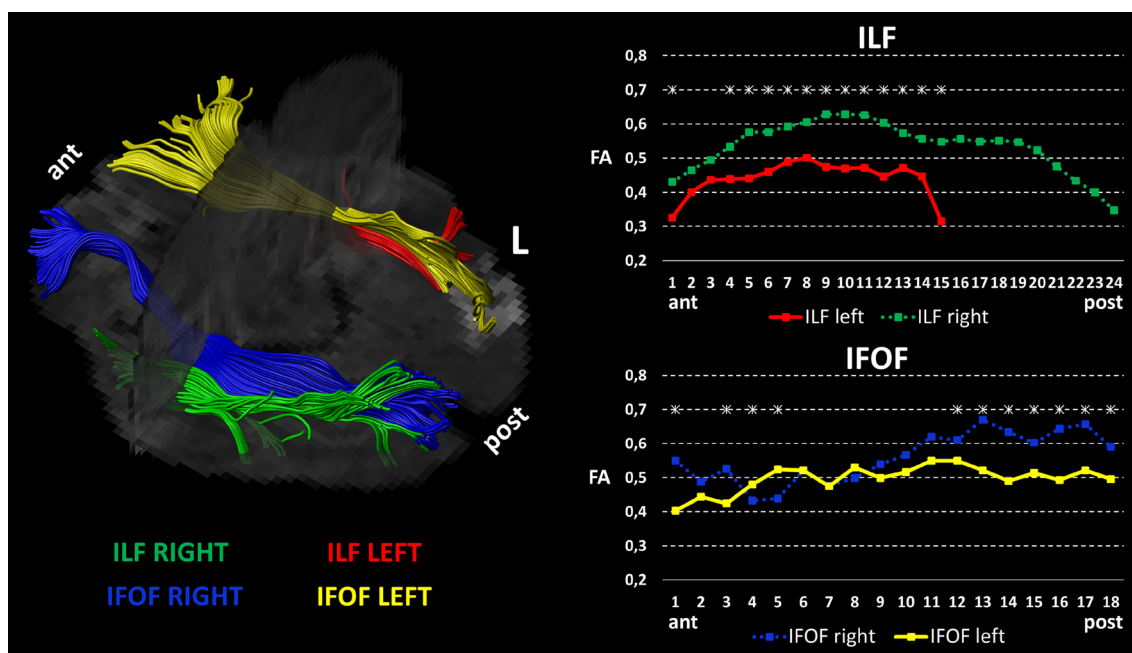


**Fig. 6** DTI tracking of the ILF and IFOF performed 18 months after resection, the lesion is hyperintense. L: left. The left ILF is interrupted due to the resection as seen on the qualitative tracking of the fiber tracts. Quantitative along tract analysis of the ILF and IFOF is shown on the right, from anterior to posterior. We cannot track the

ILF at the site of the lesion; however, anterior from this lesion, we observe decreased fractional anisotropy (FA) values, reflecting Wallerian degeneration. The IFOF shows minor degeneration close to the lesion

## Discussion

Both functional imaging and lesion studies support the theory of parallel visual processing with a dorsal stream encoding vision for action and a ventral stream supporting recognition. We describe a patient with a selective deficit in object and word processing due to a well-circumscribed lesion confined to the left occipitotemporal cortex and underlying white matter. Selective impairment of higher order visual processing can result from cortical and subcortical damage to the ventral visual stream network, which is critically involved in object and word processing.

In patient DF [4], lying at the basis of the refinement of the dual-stream hypothesis [1], occipitotemporal lesions including the LOC were bilateral and extensive, rendering a complete visual agnosia with an intact dorsal parietal stream. In patient MW, a restricted ventral occipitotemporal lesion resulted in temporary visual agnosia in the contralateral hemifield (hemi-agnosia). While performance on simple line and curve orientation was normal in the contralesional hemifield, the recognition of complex shapes was heavily impaired. RTs were markedly increased for complex visual processing and improved performance over time was paralleled by slower reaction times reflecting speed–accuracy trade-off. Complete recovery was present at 18m. The discrimination of simple visual stimuli was not affected, most

likely because the optic radiations and early visual areas were spared. It is important to note that the patient was essentially unaware of his perceptual deficit. Indeed, patients with visual hemi-agnosia can compensate by fixating on an object. Increased RTs during recovery can be explained by the recruitment of ipsi- and contralateral brain regions due to plastic reorganization. Hemi-agnosia has been reported in stroke patients with occipitotemporal cortical lesions [11–13] but without testing at different time points and without paying attention to the extent of subcortical damage.

Disorders of visual perception can, indeed, result from lesions to subcortical ventral visual pathways [22, 23]. In MW, Wallerian degeneration of the left ILF was present with decreased FA values on diffusion-based tractography. The ILF represents the major white matter tract connecting the occipitotemporal cortex, with its posterior part connecting the occipital lobe to posterior occipitotemporal areas (e.g., VWFA) and its anterior part projecting to the anterior temporal pole. Brain stimulation studies support the view that this tract subserves visual recognition in humans [24, 25]. Implication of the right ILF was also mentioned in progressive prosopagnosia [26].

In addition to hemi-agnosia, important reading difficulties were present, especially for longer words. Impaired reading could not be explained by a pure visual field deficit, since the effects of word-length are typically modest in hemianopic

dyslexia [27]. Moreover, visual field testing did not reveal hemianopia. Absolute reading speed improved markedly over time, doubling at 6w and recovering to normal at 18m. The reading deficit was attributed to a lesion of the VWFA, an area involved in word recognition, and even more so to the ILF, the white matter tract interconnecting the VWFA. The VWFA is located in the left occipitotemporal sulcus bordering the fusiform gyrus [28]. The peak activation on fMRI (MNI  $x = -43$ ,  $y = -54$ ,  $z = -12$ ) is in close relation to the area of resection [29]. Pure alexia after resection of the VWFA has been described [8] and electrical stimulation on electrodes near the VWFA can produce temporary reading deficits [30]. In MW, postoperative VWFA activations were still present anteriorly, adjacent to the lesion. Complete ILF lesions can cause pure alexia, similar to VWFA lesions [31].

Motion perception, everyday actions and performance during a visually guided grasping task were unaffected in patient MW, suggesting sparing of the dorsal visual pathway. Palinopsia, defined as the persistence or reappearance of images after cessation of a visual stimulus, has been reported in dysfunction of the ventral (e.g., face palinopsia) and dorsal visual stream (e.g., motion palinopsia), but was not present in this patient [32]. It is important to note that patients with higher order visual deficits due to occipitotemporal lesions are very rare, because the striate cortex needs to be intact with sparing of the optic radiations.

We believe that subcortical pathways should be taken into account as a potential cause of visual hemi-agnosia, a consideration that has not been reported in the previous studies. Although we propose that the ILF and its cortical projections are implicated in the deficits of MW, the relative contribution of cortical and subcortical involvement cannot be inferred from this single case study.

The current case study has several limitations. First, we did not compare RTs for left- and right-sided presentations in the complex recognition task during follow-up at each time point. The main message which we try to convey, however, is the impairment in performance not RTs, with more false alarms and less hits, not occurring on the normal side and recovering at 18 m. Theoretically, MW could have been less alert at the different time points; however, across trials and tasks, this young patient performed consistently with a low standard error of mean (in RTs), indicating a similar level of alertness and motivation. Moreover, differences in RTs were quite high, e.g., RTs at 6w were 65% higher for right- versus left-sided presentations at 1w. Second, by presenting the stimuli for a fixed duration of 800 ms and only then allowing a response, the patient could already have decided which button which he is going to press while awaiting the go-cue (stimulus offset). Since the decisional process was not delayed in any other task, and thus, we only observed consistent differences for the object recognition task which the decreased performance is based on a true

perceptual deficit. A third possible weakness of the study is the sensitivity of testing for dorsal stream involvement which could have been too low to detect subtle impairments of this pathway. A final limitation resides in the fact that we were unable to anticipate for this deficit, and therefore, no extensive preoperative data are present.

## Conclusion

Hemi-agnosia in combination with reading difficulties can occur after occipitotemporal lesions in the dominant hemisphere. Such specific lateralized higher order visual deficits result from selective damage to the ventral visual stream, which is critically involved in object and word processing.

Most visual research, in monkeys and humans, has focused on cortical areas, while the underlying subcortical network has received much less attention. We believe that the ILF can play a critical role in object perception by connecting visual areas along the ventral visual stream and that lesions of this white matter tract should be taken into consideration in agnosia patients.

**Funding** Tom Theys is a Senior Clinical Investigator of FWO Flanders (FWO 1830717N).

## Compliance with ethical standards

**Conflicts of interest** All authors report no conflict of interest.

## References

1. Goodale MA, Milner AD (1992) Separate visual pathways for perception and action. *Trends Neurosci* 15(1):20–25
2. Mishkin M, Ungerleider LG (1982) Contribution of striate inputs to the visuospatial functions of parieto-preoccipital cortex in monkeys. *Behav Brain Res* 6(1):57–77
3. Janssen P, Verhoef BE, Premereur E (2017) Functional interactions between the macaque dorsal and ventral visual pathways during three-dimensional object vision. *Cortex*. <https://doi.org/10.1016/j.cortex.2017.01.021>
4. Goodale MA, Milner AD, Jakobson LS, Carey DP (1991) A neurological dissociation between perceiving objects and grasping them. *Nature* 349(6305):154–156. <https://doi.org/10.1038/349154a0>
5. Newcombe F, Ratcliff G, Damasio H (1987) Dissociable visual and spatial impairments following right posterior cerebral lesions: clinical, neuropsychological and anatomical evidence. *Neuropsychologia* 25(1B):149–161
6. Jakobson LS, Archibald YM, Carey DP, Goodale MA (1991) A kinematic analysis of reaching and grasping movements in a patient recovering from optic ataxia. *Neuropsychologia* 29(8):803–809
7. Merigan W, Freeman A, Meyers SP (1997) Parallel processing streams in human visual cortex. *Neuroreport* 8(18):3985–3991
8. Gaillard R, Naccache L, Pinel P, Clemencau S, Volle E, Hasboun D, Dupont S, Baulac M, Dehaene S, Adam C, Cohen L (2006)

- Direct intracranial, fMRI, and lesion evidence for the causal role of left inferior temporal cortex in reading. *Neuron* 50(2):191–204. <https://doi.org/10.1016/j.neuron.2006.03.031>
9. Rezlescu C, Barton JJ, Pitcher D, Duchaine B (2014) Normal acquisition of expertise with greebles in two cases of acquired prosopagnosia. *Proc Natl Acad Sci USA* 111(14):5123–5128. <https://doi.org/10.1073/pnas.1317125111>
  10. Konen CS, Behrmann M, Nishimura M, Kastner S (2011) The functional neuroanatomy of object agnosia: a case study. *Neuron* 71(1):49–60. <https://doi.org/10.1016/j.neuron.2011.05.030>
  11. Rennig J, Karnath HO, Cornelsen S, Wilhelm H, Himmelbach M (2017) Hemifield coding in ventral object-sensitive areas—evidence from visual hemianopia. *Cortex*. <https://doi.org/10.1016/j.cortex.2017.06.011>
  12. Rennig J, Cornelsen S, Wilhelm H, Himmelbach M, Karnath HO (2017) Preserved expert object recognition in a case of visual hemianopia. *J Cogn Neurosci*. [https://doi.org/10.1162/jocn\\_a\\_01193](https://doi.org/10.1162/jocn_a_01193)
  13. Mazzucchi A, Posteraro L, Nuzzi G, Parma M (1985) Unilateral visual agnosia. *Cortex* 21(2):309–316
  14. Zeki S, Watson JD, Lueck CJ, Friston KJ, Kennard C, Frackowiak RS (1991) A direct demonstration of functional specialization in human visual cortex. *J Neurosci* 11(3):641–649
  15. Haxby JV, Horowitz B, Ungerleider LG, Maisog JM, Pietrini P, Grady CL (1994) The functional organization of human extrastriate cortex: a PET-rCBF study of selective attention to faces and locations. *J Neurosci* 14(11 Pt 1):6336–6353
  16. Tootell RB, Dale AM, Sereno MI, Malach R (1996) New images from human visual cortex. *Trends Neurosci* 19(11):481–489. [https://doi.org/10.1016/S0166-2236\(96\)10053-9](https://doi.org/10.1016/S0166-2236(96)10053-9)
  17. Popivanov ID, Jastorff J, Vanduffel W, Vogels R (2014) Heterogeneous single-unit selectivity in an fMRI-defined body-selective patch. *J Neurosci* 34(1):95–111. <https://doi.org/10.1523/JNEUROSCI.2748-13.2014>
  18. Gorgolewski K, Burns CD, Madison C, Clark D, Halchenko YO, Waskom ML, Ghosh SS (2011) Nipype: a flexible, lightweight and extensible neuroimaging data processing framework in python. *Front Neuroinform* 5:13. <https://doi.org/10.3389/fninf.2011.00013>
  19. Behzadi Y, Restom K, Liu J, Liu TT (2007) A component based noise correction method (CompCor) for BOLD and perfusion based fMRI. *NeuroImage* 37(1):90–101. <https://doi.org/10.1016/j.neuroimage.2007.04.042>
  20. Power JD, Mitra A, Laumann TO, Snyder AZ, Schlaggar BL, Petersen SE (2014) Methods to detect, characterize, and remove motion artifact in resting state fMRI. *NeuroImage* 84:320–341. <https://doi.org/10.1016/j.neuroimage.2013.08.048>
  21. Decramer T, Van Keer K, Stalmans P, Dupont P, Sunaert S, Theys T (2018) Tracking posttraumatic hemianopia. *J Neurol* 265(1):41–45. <https://doi.org/10.1007/s00415-017-8661-2>
  22. Catani M, ffytche DH (2005) The rises and falls of disconnection syndromes. *Brain* 128(Pt 10):2224–2239. <https://doi.org/10.1093/brain/awh622>
  23. ffytche DH, Blom JD, Catani M (2010) Disorders of visual perception. *J Neurol Neurosurg Psychiatry* 81(11):1280–1287. <https://doi.org/10.1136/jnnp.2008.171348>
  24. Fernandez Coello A, Duvaux S, De Benedictis A, Matsuda R, Duffau H (2013) Involvement of the right inferior longitudinal fascicle in visual hemianopia: a brain stimulation mapping study. *J Neurosurg* 118(1):202–205. <https://doi.org/10.3171/2012.10.JNS12527>
  25. Mandonnet E, Gatignol P, Duffau H (2009) Evidence for an occipito-temporal tract underlying visual recognition in picture naming. *Clin Neurol Neurosurg* 111(7):601–605. <https://doi.org/10.1016/j.clineuro.2009.03.007>
  26. Grossi D, Soricelli A, Ponari M, Salvatore E, Quarantelli M, Prinster A, Trojano L (2014) Structural connectivity in a single case of progressive prosopagnosia: the role of the right inferior longitudinal fasciculus. *Cortex* 56:111–120. <https://doi.org/10.1016/j.cortex.2012.09.010>
  27. Rubino C, Yeung SC, Barton JJ (2016) The impact of central sparing on the word-length effect in hemianopia. *Cogn Neuropsychol*. <https://doi.org/10.1080/02643294.2016.1232707>
  28. McCandliss BD, Cohen L, Dehaene S (2003) The visual word form area: expertise for reading in the fusiform gyrus. *Trends Cogn Sci* 7(7):293–299
  29. Cohen L, Lehericy S, Chochon F, Lemer C, Rivaud S, Dehaene S (2002) Language-specific tuning of visual cortex? Functional properties of the visual word form area. *Brain* 125(Pt 5):1054–1069
  30. Hirshorn EA, Li Y, Ward MJ, Richardson RM, Fiez JA, Ghuman AS (2016) Decoding and disrupting left midfusiform gyrus activity during word reading. *Proc Natl Acad Sci USA* 113(29):8162–8167. <https://doi.org/10.1073/pnas.1604126113>
  31. Epelbaum S, Pinel P, Gaillard R, Delmaire C, Perrin M, Dupont S, Dehaene S, Cohen L (2008) Pure alexia as a disconnection syndrome: new diffusion imaging evidence for an old concept. *Cortex* 44(8):962–974. <https://doi.org/10.1016/j.cortex.2008.05.003>
  32. Gersztenkorn D, Lee AG (2015) Palinopsia revamped: a systematic review of the literature. *Surv Ophthalmol* 60(1):1–35. <https://doi.org/10.1016/j.survophthal.2014.06.003>